

1 **An intermittent control model predicts the triphasic muscles activity during hand**
2 **reaching**

3 Raz Leib^{1,2}, Andrea d'Avella^{3,4}, and Ilana Nisky^{1,2}

4 ¹ Department of Biomedical Engineering, Ben-Gurion University of the Negev, Be'er
5 Sheva, Israel

6 ² Zlotowski Center for Neuroscience, Ben-Gurion University of the Negev, Be'er Sheva,
7 Israel

8 ³ Department of Biomedical and Dental Sciences and Morphofunctional Imaging,
9 University of Messina, Messina, Italy

10 ⁴ Laboratory of Neuromotor Physiology, IRCCS Santa Lucia Foundation, Rome, Italy

11

12 Acknowledgments

13 This study was conceived in collaboration with Amir Karniel who passed away
14 prematurely on June 2nd 2014. This study was supported by the Israeli Science Foundation
15 (grant #823/15) and in part by the Helmsley Charitable Trust through the Agricultural, Biological
16 and Cognitive Robotics Initiative and by the Marcus Endowment Fund both at Ben-Gurion
17 University of the Negev.

18 **Abstract**

19 There are numerous ways to reach for an apple hanging from a tree. Yet, our motor system
20 uses a specific muscle activity pattern to generate reaching movements that have similar
21 characteristics. For many decades, we know that this pattern features activity bursts and
22 silent periods. We suggest that these bursts are a strong evidence against the common view
23 that the brain continuously controls the commands to the muscles. Instead, we suggest a
24 model that changes these commands in a discrete way. We use unsupervised machine
25 learning to identify transitions in the state of the muscles, and show that fitting a discrete
26 model to the kinematics of movement using only one parameter predicts the transitions in
27 the state of the muscles. Such discrete controller suggests that the brain reduces the
28 complexity of the motor control problem as well as the wear-and-tear of the muscles by
29 sending commands to the muscles at sparse times. Identifying this discrete controller can
30 be applied in the control of prostheses and physical human-robot interaction systems such
31 as exoskeletons and assistive devices.

32 **Introduction**

33 During multi-joint arm movement, there is activity alteration between agonist and
34 antagonist muscles groups. For hand point-to-point reaching movements, the muscles
35 exhibit a unique activation pattern which consist of switching between activity bursts and
36 silent periods, known as the tri-phasic muscles activity pattern (Hallett, Shahani et al. 1975,
37 Flanders 1991, Flanders, Pellegrini et al. 1996). These patterns characterize muscle activity
38 in different types of movements (Bizzi, Kalil et al. 1971, Hallett and Marsden 1979,
39 Mustard and Lee 1987, Hoffman and Strick 1990), suggesting that a central program
40 controls the precise timing of switching (Sanes and Jennings 1984). Yet, the origin of such
41 central program is still unknown. Here, we show that an intermittent control model can
42 explain these activity patterns during hand reaching.

43 Many studies aimed to reveal the nature of such central program by examining kinematic
44 characters of the hand during point-to-point reaching motion. While there are various ways
45 to reach from one point to another, these movements are typically made using a straight-
46 line path with a stereotypic bell-shaped velocity trajectory (Morasso 1981). These motion
47 features suggest that a simple control mechanism is responsible for generating such
48 movement. To explain this mechanism, different models based on optimal control theory
49 were proposed, such as minimum jerk (Flash and Hogan 1985), minimum joints torque
50 (Uno, Kawato et al. 1989), or minimum muscle tension change (Dornay, Uno et al. 1996).
51 The difference between these models is that each model has different prediction regarding
52 the control signal that is used to generate motion. This control signal is assumed to serve
53 as the basis for the central program that is responsible for muscle activation and eventually
54 hand motion.

55 Most of the optimal control models that describe hand movement are based on continuously
56 changing control signal that generates the motion. However, the abrupt changes in the
57 muscles activity as seen in the EMG signals suggest that the control signal is a result of an
58 intermittance based control mechanism. Such mechanism would occasionally change the
59 control signal at certain sparse points in time according to a control law.

60 Recently, an intermittent optimal control based model was suggested to explain the
61 kinematic of the trajectory of reach (Ben-Itzhak and Karniel 2008) and object manipulation
62 (Leib and Karniel 2012) movements. This model is based on minimizing hand acceleration
63 which results in a piecewise constant control signal (Minimum Acceleration with
64 Constraints model). The resulting control signal is characterized by two transitions between
65 control values that generate motion (Ben-Itzhak and Karniel 2008). Here, we show that this
66 intermittence optimal control based model that describes the kinematics of hand motion
67 can also explain the timing of the muscles activity. We compare the timing of transitions
68 in the control signal as predicted by this model with the timing of transitions in muscles
69 activity, and provide a possible explanation to the tri-phasic muscle pattern.

70 The previously proposed minimum muscle tension model predicts muscle activity
71 alteration between the agonist and antagonist muscles during reaching, but the predicted
72 pattern is different from the tri-phasic pattern (Dornay, Uno et al. 1996). In contrast, we
73 show here that the MAC control signal predicts alterations in muscle activity that are
74 similar to the observed tri-phasic pattern. This bang-bang control signal, transmitted from
75 the brain, serves as the neural drive for generating muscle activity (Dowling 1992) which
76 will result in hand movement. Due to Electromechanical delays between the muscle
77 activity onset and movement onset (Norman and Komi 1979), we expected some
78 differences between the transitions times in the control signal, which we derive from
79 kinematic data, and the transitions in EMG signals. However, we show that adding this
80 constant delay to our predictions drastically improves the fit.

81 Results

82 We used EMG signals and hand position data that were recorded during center-out and
83 out-center reaching movements in a previous study (d'Avella, Portone et al. 2006).
84 Movements were made between a center position and eight different targets positioned
85 evenly on a circle. An example for one movement is depicted in the upper panel of Figure
86 1A. All movements were characterized by sigmoidal position trajectories and bell shaped
87 velocity trajectories. We extracted the movement duration and movement length from these
88 signals, and used these parameters to calculate the Minimum Acceleration with Constraints
89 (MAC) model trajectory. This model minimizes the acceleration of the hand while
90 constraining the jerk value, and yields a piecewise-constant jerk trajectory with two switch
91 times between jerk values. We fitted the optimal MAC predicted position to the recorded
92 position signal by finding the value of the jerk that minimizes the error between model's
93 prediction and actual position. Using this fitting process between the MAC model predicted
94 position trajectory to the actual hand position trajectory allowed for extracting the
95 transition times t_1^{MAC} and t_2^{MAC} from the fitted control signal (Figure 1A, middle panel). We
96 call these transitions *MAC-predicted transitions*. This process is depicted in the middle
97 panel of Figure 1A. In addition, during the movement, EMG was recorded from 17-18
98 muscles. Using an algorithm of multiple point-change detection implemented using the
99 Markov Chain Monte Carlo (MCMC) method, we detected the transition times t_1^{EMG} and
100 t_2^{EMG} in each EMG signal independently from the kinematics information. We call these
101 transitions *EMG-detected transitions*.

102 An example for reaching movement and EMG recorded from one muscle during motion is
103 depicted in Figure 1A (bottom panel). In this example, we found that the EMG-detected
104 transitions times of the EMG signal are similar to the MAC-predicted transitions times of
105 the MAC model control signal. An example of the transition times within the three-phase
106 pattern in all the muscles that were recorded during a single movement is depicted in Figure
107 1B. For many of the muscles, the EMG-detected transitions were remarkably coincident
108 with the MAC-predicted transition times. For example, this was true for the TrLat, DeltA,
109 TrapMed, and TeresMaj, and very close also for BicLong and Brac. However, for some of
110 the muscles, the MAC-predicted transitions times did not match the EMG-detected

111 transitions times, but rather it seemed that both transitions were shifted together,
112 predominantly towards earlier in time.

113 A correlation analysis between MAC-predicted transitions and EMG-detected transitions
114 for all muscles of a single participant across all trials is depicted in Figure 2A. In this
115 example, the MAC-predicted and EMG-detected transitions are correlated for both t_1 and
116 t_2 separately and together. However, there is relatively large variance in the ability of the
117 MAC model to predict the EMG transitions, as indicated by the point scatter in each panel.
118 An analysis of the correlation coefficients across all participants confirmed this observation
119 (Figure 2B). We found a correlation coefficient of 0.47 ± 0.17 (mean \pm STD) between t_1^{MAC}
120 and t_1^{EMG} , a correlation coefficient of 0.52 ± 0.18 between t_2^{MAC} and t_2^{EMG} , and a correlation
121 coefficient of 0.84 ± 0.08 when both transition times are analyzed together.

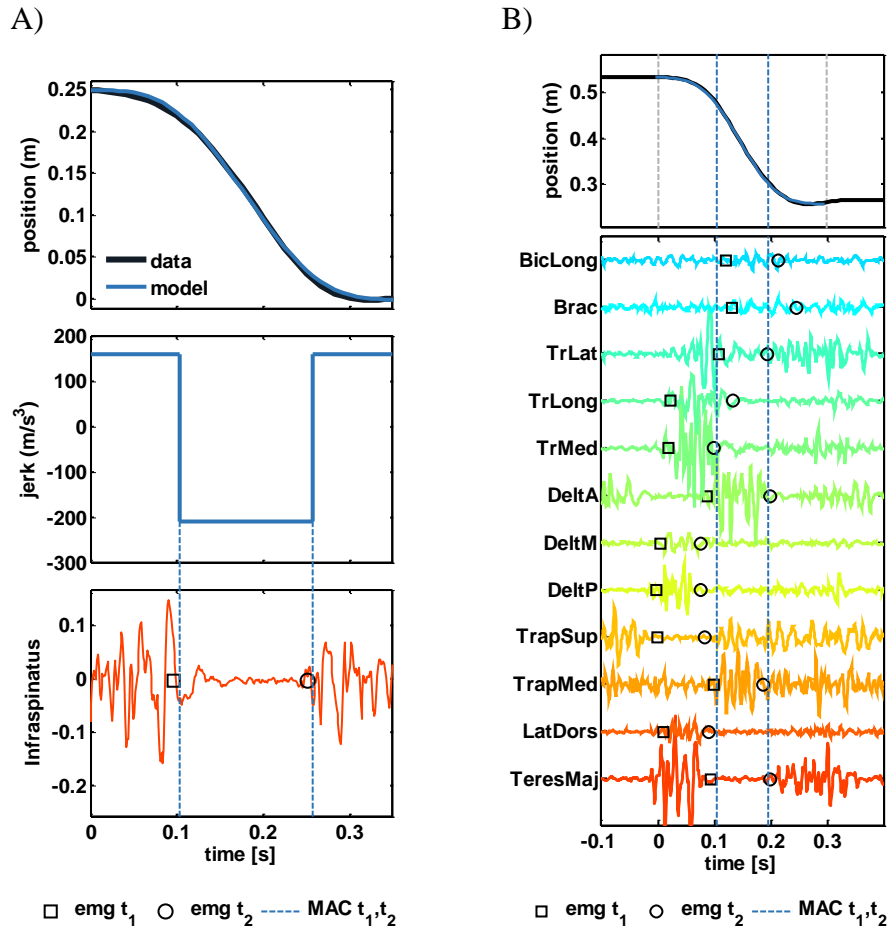


Figure 1: Examples for EMG transitions times predicted by the transition times of the MAC model control signal.

A) Example for matching between MAC transitions and EMG transitions. Upper panel represents an example of a position trajectory (black line) and the fitted MAC model to this data (blue line). Middle panel represents the model's jerk control signal that was used to generate the model's position trajectory. Here we marked the transition times, t_1^{MAC}, t_2^{MAC} , using a dashed blue lines. Bottom panel represents an EMG signal from one muscle (red line). The first transition in this signal, t_1^{EMG} , is represented by a black square, and the second transition, t_2^{EMG} , is represented by a black circle.

B) Example for matching between the transitions times observed in the activity of multiple muscles during a single reaching movement and the MAC-predicted transition times. Each row represent an EMG signal recorded from a single muscle whose name is indicated on the left side. The MCMC detected transitions in EMG signals (EMG-detected) are marked as in (A). The two vertical blue lines represent the MAC-predicted transitions extracted from the MAC model that were fitted to this movement. The two vertical gray lines represent the initial and end times of the movement.

122

123

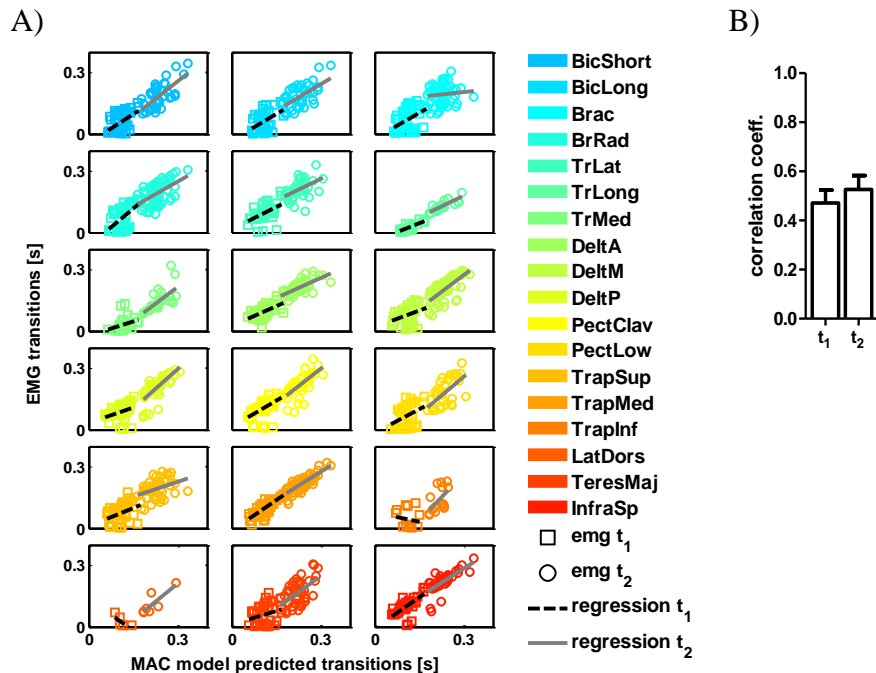


Figure 2: Correlation analysis between the MAC predicted transitions and EMG detected transitions.

A) Representative correlation between MAC-predicted and EMG-detected transitions for all movement of a single participant. Each panel represents the EMG-detected transitions as a function of MAC-predicted transitions for all muscles. The information of each movement is represented using one square and circle. Empty squares represent the first transition data (t_1) and circles represent the second transition data (t_2). In each panel, the fitted regression line for the first transition data is represented using a dashed black line, and the fitted regression line for the second transition is represent using a solid gray line. For some muscles the predictions of the MAC model match the transitions in the EMG signal; however, there is large variability around the regression line.

B) Mean correlation coefficient for all muscle across all participants. The mean correlation coefficient for the first transition and second transition is marked using an unfilled bar, and the mean value for the second transition is marked using a filled bar. Error bars represent 95% confidence intervals calculated using a t-distribution.

124

125 We reasoned that the variability in the ability of the model to predict the accurate timing
 126 of transition is a result of temporal shifting of the tri-phasic activity pattern between
 127 different muscles (Flanders 1991, Flanders, Pellegrini et al. 1994, Flanders, Pellegrini et
 128 al. 1996). These shifts are apparently an important variable for the motor system (Karst
 129 and Hasan 1991, Hoffman and Strick 1999) and ranged between 30 and 100 ms (Cavanagh
 130 and Komi 1979). Previous studies captured such shifts using time-varying synergies

131 (d'Avella, Portone et al. 2006). For example, in Figure 1B, we show that some muscles are
132 activated before movement starts. Since the MAC model is fitted to the hand position
133 signal, it cannot accurately predict these shifted transitions. However, if indeed one central
134 program is used to activate muscles but it arrives to different muscles at different times, we
135 can eliminate the effect of the different temporal shifts between the muscles by looking at
136 the difference in the times of the transitions. One way of looking at the time differences is
137 examining the temporal difference between the first activity transitions in the EMG signal
138 and the MAC control signal ($\Delta t_1 = t_1^{MAC} - t_1^{EMG}$), and then compare it with difference
139 between the second activity transitions in the same signals ($\Delta t_2 = t_2^{MAC} - t_2^{EMG}$). If indeed
140 the EMG activation is correlated with the MAC control signal, we expect to see that the
141 two differences are similar ($\Delta t_1 = \Delta t_2$). To examine this, we fitted a two-degrees of freedom
142 regression line between Δt_1 and Δt_2 . If the two values are similar, we expect to get a
143 regression line with a unit slope and a zero intercept. Alternatively, different result will
144 mean that the two values are not linked, suggesting that the MAC-predicted transitions
145 cannot predict the EMG-detected transitions. Figure 3A shows an example for this analysis
146 for all the muscles of one participant. In this example, we found that all the regression slope
147 values were close to 1, and that the intercept values were close to 0. Generally, we found
148 that the mean value of the slope was 0.87 ± 0.17 (mean \pm STD) and the mean value of the
149 intercept was -0.003 ± 0.005 . These results support the idea that the EMG transitions are
150 correlated with the MAC transitions.

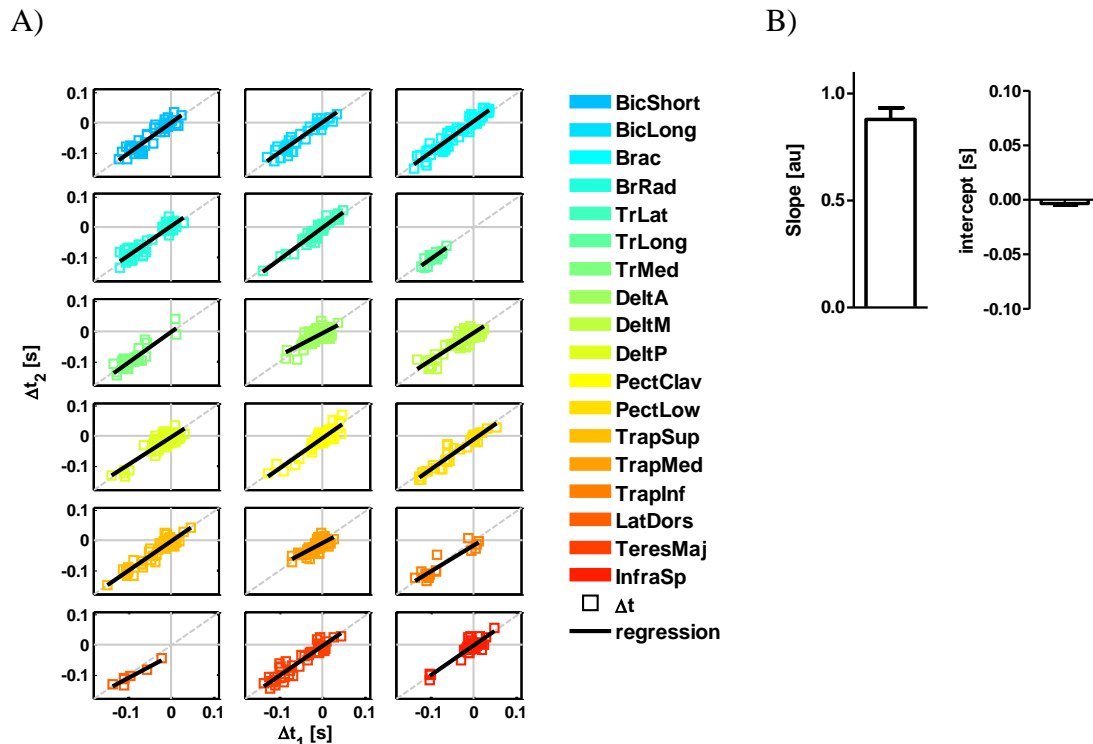


Figure 3: correlation between temporal difference between EMG-detected transitions and MAC-predicted transitions.

A) Differences analysis of a single participant movements. Each panel represents the difference between the second EMG-detected transition and the second MAC-predicted transition ($\Delta t_2 = t_2^{MAC} - t_2^{EMG}$) as a function of this difference but for the first transitions ($\Delta t_1 = t_1^{MAC} - t_1^{EMG}$). Each movement is represented using a single colored square. The black line in each panel represents the regression line that was fitted to the data. By comparing this regression lines to an ideal correlation between the variables (dashed gray line) we found that the two values are similar to each other

B) Mean slope and intercept values for all muscles across all participants. Error bars represent 95% confidence interval estimated using a t-distribution.

151

152 A different approach to understand the effect of the temporal shift on the ability of the
 153 MAC model to predict the tri-phasic transitions timing is to find the temporal shift of the
 154 activity pattern for each muscle. To do so, we extracted sets of delay values that generated
 155 the highest correlation coefficient between EMG-detected transitions (t_1^{EMG}, t_2^{EMG}) and
 156 MAC-predicted transitions (t_1^{MAC}, t_2^{MAC}) for all muscles. Each set was assembled from one
 157 to ten delay values. This means that we extracted ten sets of delay values, where the first
 158 one included only one delay value, and the 10th set included ten delay values. Using a single
 159 delay value from the set, we shifted both t_1^{EMG}, t_2^{EMG} EMG transitions. The single delay

160 value that was picked from the set was the one that minimizes the temporal difference
161 between the EMG-detected transitions and MAC-predicted transitions. An example for the
162 result of such “shift-corrected” analysis using the 5th set of five different delay values is
163 depicted in Figure 4A: we show the correlation between EMG-detected transitions and
164 MAC-predicted transitions for a single participant after optimizing five different possible
165 shifts. We found that increasing the number of possible delay values increased the
166 correlation between the EMG-detected transitions and MAC-predicted transitions (Figure
167 4B). This increase occurs simultaneously for both EMG transitions since we observed that
168 the difference between the first transition in the EMG and MAC control signal ($t_1^{MAC} - t_1^{EMG}$
169) is very similar to the difference between the second transitions ($t_2^{MAC} - t_2^{EMG}$). This means
170 that both EMG-detected transitions can be aligned with the two MAC-predicted transitions
171 using a simple shift. On average, we can achieve a strong correlation (a correlation
172 coefficient > 0.7) between EMG-detected transitions and MAC-predicted transitions timing
173 using five delay values.

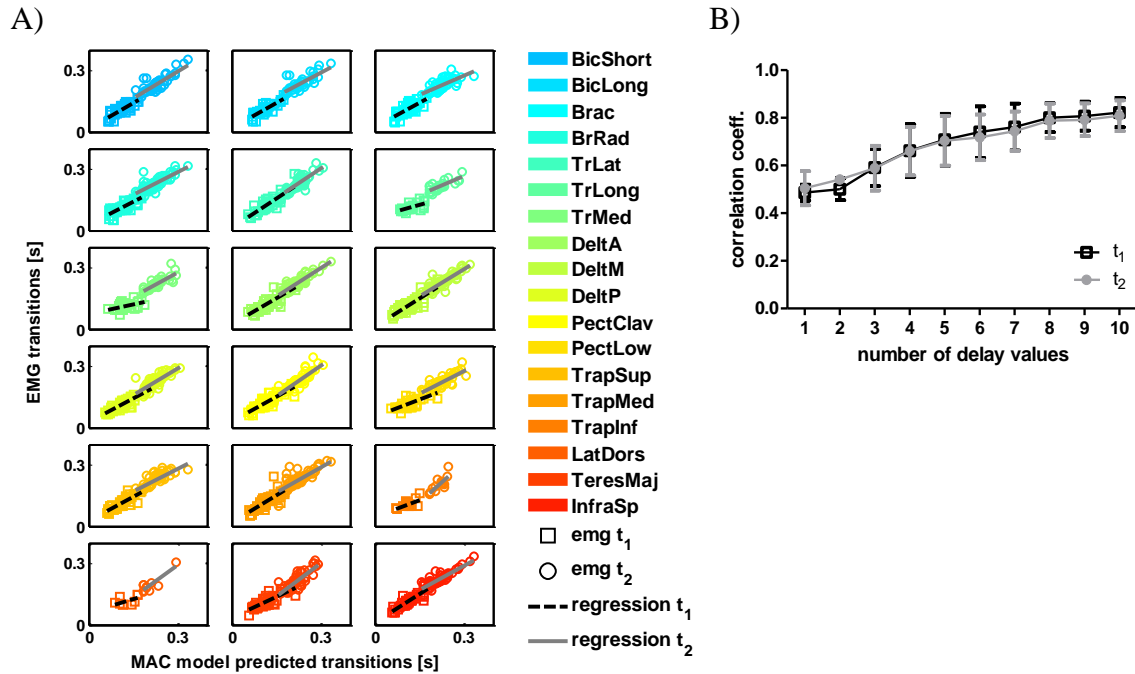


Figure 4: Correlation analysis between the MAC predicted transitions and EMG detected transitions with added temporal shifts.

A) Same example as in Figure 2A with shifted EMG transitions. We shifted the two EMG transitions detected in each movement by a single value out of five delay possibilities. Following this shift we observed an increase in correlation for both the first and second transitions. All notation are similar to Figure 2A.

B) The correlation coefficient value as a function of possible shifts used on the EMG transitions. Allowing more delay values to shift the EMG transitions increased the correlation between the MAC predicted transitions and the EMG transitions. In all the delay sets, the same shift was applied on both t_1 and t_2 of the same muscle.

174

175

176 **Discussion**

177 In this study we suggest that an intermittent optimal control based model can predict both
178 transitions in the state of the muscles as well as the kinematic features of the hand during
179 point-to-point reaching movement. We show that the timing of transitions in the piecewise-
180 constant control signal used to describe the hand trajectory are synchronized with the
181 transitions times that are observed in EMG signals. These results suggest that the muscles
182 are activated using a variation of this single piecewise-constant signal. We observed a
183 temporal shift of the tri-phasic pattern that suggests that the activation signal arrives to the
184 muscles at different times during the movement. Nevertheless, we found that the time that
185 elapses between the first notable transition in muscles activity and the transition in the
186 activation signal is similar to the time elapses between the second transitions in these
187 signals.

188 Previous studies struggled with the question how the motor system generates muscle
189 activity pattern. In many conditions, the CNS generates muscle activity and ultimately hand
190 motion by specifying a centrally programmed motor command (Sanes and Jennings 1984).
191 We show that the MAC model explains the connection between movement characteristics
192 and the pattern of muscles activity. Therefore, we suggest that it can be a possible candidate
193 control policy for such central mechanism. Previous studies examined the relations
194 between the temporal profiles of agonist-antagonist muscle system during reaching
195 movement and showed that the agonist initial activity is terminated before peak velocity
196 while the burst of the antagonist muscle initiate before peak velocity (Brown and Cooke
197 1990). Such activity profile is well explained by the MAC model where the first transition
198 time in the control signal occurs prior to the peak velocity time. Another feature of the
199 model is the jerk constraint which can generate different transitions times in the control
200 signal without changing any other movement constraints such as duration or length. Thus,
201 by changing the jerk constraint we can generate short and long EMG bursts patterns that
202 are similar to the EMG patterns with different bursts durations that were found during
203 reaching movements with the same duration and length but to different positions in space
204 (Flanders, Pellegrini et al. 1994) or during movements with external load attached to the
205 hand (Hong, Corcos et al. 1994).

206 To summarize these results, we suggest a control scheme (Figure 5) based on intermittent
207 control (Karniel 2013). In this scheme, the brain sends pulse-like commands at specific
208 times to generate the hand movement, as predicted by the control signal of the MAC model.
209 This signal is then transformed into muscle activation profiles. Previous studies showed
210 that this transformation can be described as a low pass filter (Crosby 1978, Patla, Hudgins
211 et al. 1982, Dowling 1992). The resulted muscle activation signal is integrated to produce
212 a momentum at the joint (Coggshall and Bekey 1970). The relation between the muscle
213 activation and muscle momentum depends on different factors such as the muscle current
214 length (Gordon, Huxley et al. 1966). In addition, these muscle activations patterns can be
215 temporally shifted in order to create a specific spatiotemporal organization of muscle
216 activity, or time-varying muscle synergies (d'Avella, Portone et al. 2006). Indeed, a time-
217 varying synergy prescribes the activation of different muscles at different times, thus
218 predicting different transition times in individual muscles with respect to the synergy onset.
219 This provides an explanation to the temporal shift of the transitions in the control signal
220 between groups of muscles that we found in this study. Finally, using the muscle
221 momentum and considering the limb moment of inertia, we can calculate the angular
222 velocity of the joint.

223

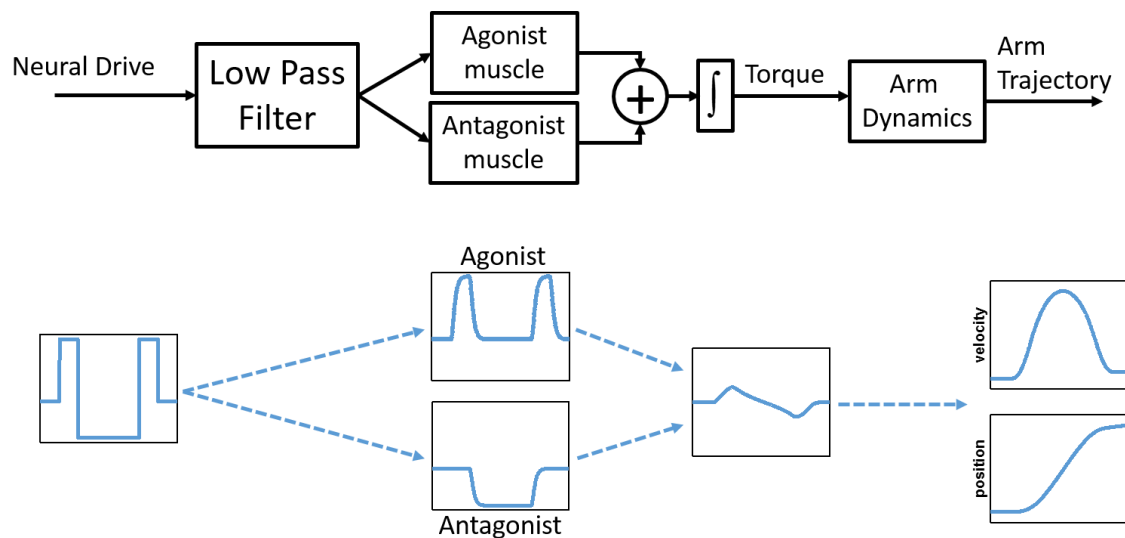


Figure 5: A sketch of the muscle activation system based on intermittent control. The brain is responsible for generating arm movements by sending a piecewise constant control

signal which is filtered using a low pass filter and then transformed into muscle activation pattern based on the state of the muscle. The produced torque can be simulated by integrating this electrical activity and used to generate the arm movement. In this study, we showed that the transitions in the control signal as predicted by the MAC model hand movement match the transitions in the EMG activity, suggesting that the brain could use the MAC criteria to generate reaching movement. Bottom flow chart shows simulated signals of a single link arm movement using an agonist-antagonist muscle system activated using the MAC control signal. In each panel we plot the signals after the different transformations starting from a piecewise-constant MAC signal

224

225 There is a wide range of evidence for the existence of intermittent control in the motor
226 system (Gawthrop, Loram et al. 2011). Many studies examined the intermittent nature of
227 movements during tracking (Navas and Stark 1968, Miall, Weir et al. 1986, Miall, Weir et
228 al. 1987, Neilson, Neilson et al. 1988, Hanneton, Berthoz et al. 1997, Squeri, Masia et al.
229 2010, Gawthrop, Loram et al. 2011) where it was suggested that a refractory period of the
230 central nervous system (Neilson, Neilson et al. 1988) or exceeding a threshold of tracking
231 error (Miall, Weir et al. 1986, Hanneton, Berthoz et al. 1997, Gawthrop 2010) is
232 responsible for generating movements. In addition, Intermittent control is also evident
233 during isometric force tasks (Slifkin, Vaillancourt et al. 2000, Vaillancourt, Mayka et al.
234 2006), and tasks that require tracking a target while experiencing forces (Squeri, Masia et
235 al. 2010), switching between motion and force control (Venkadesan and Valero-Cuevas
236 2008), rhythmic movements (Doeringer and Hogan 1998), object manipulation (Gawthrop,
237 Loram et al. 2009, Loram, Gollee et al. 2011, Leib and Karniel 2012), in handwriting and
238 drawing (Viviani and Terzuolo 1982, Schenk, Walther et al. 2000), and in catching
239 (D'Andola, Cesqui et al. 2013). Here, we suggest that the intermittent control policy is
240 evident even in the simplest reach movements, and that it provides a compelling
241 explanation to the well known triphasic muscle activity pattern.

242 To further support the results presented here, we suggest examining the muscle activity
243 pattern during more complex movement, such as via-point movements, while developing
244 related computational models based on intermittent control. In addition, our predictions
245 may be tested using neural activity at higher levels of the motor system hierarchy. Indeed,

246 different studies found evidence for intermittent control strategy such as in the case of the
247 bursting activities separated by pauses in Pukinje cells (Loewenstein, Mahon et al. 2005).

248 In this study we provide a link between the discrete nature of muscle activity and the
249 continuous signals that characterize hand movement. Using an intermittent control model
250 that describe the hand trajectory during reaching movements we were also able to capture
251 the transitions in the state of the muscles during the movement. This result suggests that
252 the motor system uses discrete control based approach to generate movement instead of a
253 continuous control approach which is considered by many to be a fundamental way to
254 describe the characters of the motor system.

255 Understanding whether the motor system employ intermittent control to generate motion
256 can have potential implications. For example, it can be useful in simplifying the control of
257 prostheses and other physical human-robot interaction system. Intermittent control is
258 especially attractive in simplifying control when computational resources are limited and
259 in conditions with delay, such as in the case of online processin of information during the
260 control of smart prosthesis. Moreover by comparing the timing of the transitions events
261 between impaired and unimpaired populations, we can learn about the origin (central or
262 peripheral) of specific motor diseases, which can be useful for developing patient-tailored
263 physical therapy and other forms of treatment of motor pathologies.

264 **Methods**

265 We used data previously published by d'Avella et al. (d'Avella, Portone et al. 2006). The
266 dataset we analyzed included trajectories of three participants that made center-out and out-
267 center hand movement to eight equally spaced targets positioned on a 30 cm circle. Each
268 participant made five center-out and five out-center movements in the frontal plane
269 between the center and each of the eight targets summing to a total of 80 movements.
270 During the movement, endpoint trajectory and the EMG activity of 17-18 muscles (as
271 shown in Table 1, for more details on the experimental design and apparatus see the original
272 work by d'Avella et al.) were recorded.

273 Table 1. Summary of muscles recorded for each subject. Subjects' number are based on the
274 numbers reported in the original work.

Muscle	Subjects		
	3	6	7
Biceps brachii, short head (BicShort)	+	+	+
Biceps brachii, long head (BicLong)	+	+	+
Brachialis (Brac)	+	+	+
Pronator Teres (PronTer)	+	+	-
Brachioradialis (BrRad)	+	+	+
Triceps brachii, lateral head (TrLat)	+	-	+
Triceps brachii, long head (TrLong)	+	+	+
Triceps brachii, medial head (TrMed)	+	+	+
Deltoid, anterior (DeltA)	+	+	+
Deltoid, medial (DeltM)	+	+	+
Deltoid, posterior (DeltP)	+	+	+
Pectoralis major, clavicular (PectClav)	+	+	+
Pectoralis major, sternal (PectInf)	-	+	+
Trapezius, superior (TrapSup)	+	+	+
Trapezius, medial (TrapMed)	+	-	+
Trapezius, inferior (TrapInf)	-	+	+
Latissimus dorsi (LatDors)	+	+	+
Teres Major (TeresMaj)	+	+	+
Infraspinatus (InfraSp)	+	+	+

275

276

277

278 *Minimum Acceleration with Constraints model*

279 To extract the predicted transitions from the hand position signal, we used the Minimum
 280 Acceleration with Constraints (MAC) model. This model for reaching movement is based
 281 on minimizing the hand acceleration during motion while constraining the maximum value
 282 of the hand jerk u_m . The solution to this problem is a straight line, of the following form

283
$$\underline{x}(t) = \underline{x}(0) + \frac{1}{L} r(t) \cdot (\underline{x}(T) - \underline{x}(0))$$

284 where $\underline{x}(0)$ and $\underline{x}(T)$ are the initial point and end point of the movement respectively. L
 285 is the length of the movement and $r(t)$ is a time dependent function consist of three
 286 segments of third order polynomials

$$(1) \quad r(t) = \begin{cases} \frac{1}{6} u_m t^3 & 0 \leq t < t_1^{MAC} \\ \frac{1}{6} c_0 t^3 - \frac{1}{2} c_1 t^2 + c_2 t + c_3 & t_1^{MAC} \leq t < t_2^{MAC} \\ \frac{1}{6} u_m t^3 - \frac{1}{2} u_m T \cdot t^2 + \frac{1}{2} u_m T^2 \cdot t + L - \frac{1}{6} u_m T^3 & t_2^{MAC} \leq t \leq T \end{cases}$$

287 where

$$(2) \quad \begin{aligned} c_0 &= \frac{-24u_m \cdot L}{u_m \cdot T^3 - 24 \cdot L + \sqrt{u_m \cdot T^3 (u_m \cdot T^3 - 24 \cdot L)}} \\ c_1 &= \frac{-12u_m \cdot L \cdot T}{u_m \cdot T^3 - 24 \cdot L + \sqrt{u_m \cdot T^3 (u_m \cdot T^3 - 24 \cdot L)}} \\ c_2 &= \frac{(12 \cdot L - u_m \cdot T^3) \sqrt{u_m \cdot T} + u_m \cdot T^2 \sqrt{u_m \cdot T^3 - 24 \cdot L}}{4 \sqrt{u_m \cdot T^3 - 24 \cdot L}} \\ c_3 &= \frac{(6 \cdot L - u_m \cdot T^3) \sqrt{u_m \cdot T^3 - 24 \cdot L} + (u_m \cdot T^3 - 18 \cdot L) \sqrt{u_m \cdot T^3}}{12 \sqrt{u_m \cdot T^3 - 24 \cdot L}} \end{aligned}$$

288 and

$$(3) \quad \begin{aligned} t_1^{MAC} &= \frac{T}{2} \left(1 - \sqrt{\frac{u_m \cdot T^3 - 24 \cdot L}{u_m \cdot T^3}} \right) \\ t_2^{MAC} &= \frac{T}{2} \left(1 + \sqrt{\frac{u_m \cdot T^3 - 24 \cdot L}{u_m \cdot T^3}} \right) \end{aligned}$$

289 This model predicts two transitions in the control signal at times t_1^{MAC}, t_2^{MAC} (Figure 1A).

290 To fit the model to the hand movement data we first used the recorded velocity signal to
291 identify movement initiation and end times. Using these times we extracted the initial and
292 target positions of the motion as well as the duration of the movement (T). Following
293 finding the parameters, we fitted the MAC model by optimizing the jerk constraint in such

294 way that the Root Mean Square Error ($RMSE = \sqrt{\frac{1}{T} \sum_{i=1}^T (x_i^{data} - x_i^{model})^2}$) between the
295 recorded position signal (x^{data}) and model's position signal (x^{model}) will be minimized.

296 Using the jerk constraint from the position RMSE optimization process, movement
297 duration and length allowed us to find the two transitions times predicted by the MAC
298 model according to equation (3).

299 *Detecting transitions in EMG signal*

300 To detect transitions in the EMG signal, we used an algorithm of multiple point-change
301 detection which is based on a Bayesian approach and implemented using the Markov Chain
302 Monte Carlo (MCMC) method (Lavielle and Lebarbier 2001). The algorithm marked the
303 transitions in the EMG signal based on changes in the mean and variance of the signal
304 magnitude. We considered only the transitions within the three-phase pattern. In some
305 cases, such as for the TereMaj or the TrLat muscles depicted in Figure 1B,
306 the algorithm detected additional transitions of the start and end of the three-phase pattern.
307 In such cases, we omitted the two additional transitions and considered only the transitions
308 between the first phase and third phase of the pattern.

309

310 *Data analysis*

311 For each movement, we identified the active muscles that showed significant EMG activity
312 by setting a threshold of EMG magnitude (average magnitude > 0.05 μ V). We then extracted

313 the activity transitions in the EMG signal of each muscle (t_1^{EMG}, t_2^{EMG}) and the transitions
314 in control signal of the fitted MAC model (t_1^{MAC}, t_2^{MAC}). This procedure was repeated for
315 all movements. We examined the overall ability of the MAC model to predict transitions
316 in the EMG signals by fitting a regression line between the MAC predicted transitions
317 timing and the EMG detected transitions timing. We used separate regression lines for the
318 first transitions, i.e. between t_1^{MAC} and t_1^{EMG} , and for the second transition, i.e. between t_2^{MAC}
319 and t_2^{EMG} .

320 Since different muscle groups exhibit activity pattern at different stages of the movement,
321 and even before movement initiated (Moran and Schwartz 1999), understanding whether
322 the transitions in the EMG signal match the transitions in MAC control signal require
323 temporal shift in order to be synchronized between them. We can formulate this temporal shift
324 as the temporal difference between the first transition in the EMG and MAC control signal,
325 i.e. $\Delta t_1 = t_1^{MAC} - t_1^{EMG}$, or between the second transition, i.e. $\Delta t_2 = t_2^{MAC} - t_2^{EMG}$. If the EMG
326 transitions are a temporally shifted version of the MAC transitions this means that Δt_1
327 should have similar value to Δt_2 . To quantify this, we fitted a two degrees of freedom
328 regression line to the data with Δt_1 as the independent variable and Δt_2 as the dependent
329 variable. A perfect match between the two differences will result in a regression line with
330 unit slope and zero intercept.

331 In addition, we estimated the optimal temporal shift between the EMG transitions and
332 MAC transitions. To do so, we searched for sets of shifts values starting from a single shift
333 to a set of ten shift values. To find the optimal shift values for each set, we varied the values
334 of the shifts between -300ms and 300ms with jumps of 1ms. For example, for a set of three
335 shifts we started the search from the possible shifts vector [-298, -299, -300] and ended the
336 search at [298, 299, 300] covering all possible combinations. To each MAC predicted
337 transitions pair, t_1^{MAC}, t_2^{MAC} , we added one value from a candidate shifts vector. The shift
338 chosen was the shift that had the smallest absolute distance between the MAC predicted
339 transitions and the EMG detected transitions, t_1^{EMG}, t_2^{EMG} , i.e.

340 $distance = |t_1^{EMG} - t_1^{MAC}| + |t_2^{EMG} - t_2^{MAC}|$. We repeated this calculation for all muscles and
341 for all movements. For each possible shifts vector we calculated the correlation between
342 MAC-predicted transitions and EMG-detected transitions for each muscle and averaged

343 the correlation values. We chose the optimal shifts vector as the vector that gave the highest
344 average correlation value. We repeated this this procedure for each participant. Here we
345 present the results for the first ten sets. Increasing the number of possible shift values will
346 increase the correlation value between the MAC-predicted transitions and EMG-detected
347 transitions since there will be more possible shift values to choose from. Ultimately, we
348 can find the optimal shift for every MAC-predicted transitions and EMG-detected
349 transitions pair by increasing the number of possible values in the set.

350 **References**

- 351 Ben-Itzhak, S. and A. Karniel (2008). "Minimum acceleration criterion with constraints
352 implies bang-bang control as an underlying principle for optimal trajectories of arm
353 reaching movements." Neural Computation **20**(3): 779-812.
- 354 Bizzi, E., R. E. Kalil and V. Tagliasco (1971). "Eye-head coordination in monkeys:
355 evidence for centrally patterned organization." Science **173**(3995): 452-454.
- 356 Brown, S. H. and J. D. Cooke (1990). "Movement-related phasic muscle activation. I.
357 Relations with temporal profile of movement." Journal of Neurophysiology **63**(3): 455-
358 464.
- 359 Cavanagh, P. R. and P. V. Komi (1979). "Electromechanical delay in human skeletal
360 muscle under concentric and eccentric contractions." European Journal of Applied
361 Physiology and Occupational Physiology **42**(3): 159-163.
- 362 Cogshall, J. C. and G. A. Bekey (1970). "EMG-force dynamics in human skeletal
363 muscle." Medical and biological engineering **8**(3): 265-270.
- 364 Crosby, P. A. (1978). "Use of surface electromyogram as a measure of dynamic force in
365 human limb muscles." Medical and Biological Engineering and Computing **16**(5): 519-
366 524.
- 367 D'Andola, M., B. Cesqui, A. Portone, L. Fernandes, F. Lacquaniti and A. d'Avella (2013).
368 "Spatiotemporal characteristics of muscle patterns for ball catching." Frontiers in
369 Computational Neuroscience **7**(107).
- 370 d'Avella, A., A. Portone, L. Fernandez and F. Lacquaniti (2006). "Control of fast-reaching
371 movements by muscle synergy combinations." The Journal of neuroscience **26**(30): 7791-
372 7810.
- 373 Doeringer, J. A. and N. Hogan (1998). "Intermittency in Preplanned Elbow Movements
374 Persists in the Absence of Visual Feedback." Journal of Neurophysiology **80**(4): 1787-
375 1799.
- 376 Dornay, M., Y. Uno, M. Kawato and R. Suzuki (1996). "Minimum muscle-tension change
377 trajectories predicted by using a 17-muscle model of the monkey's arm." Journal of Motor
378 Behavior **28**(2): 83-100.
- 379 Dowling, J. J. (1992). "The effect of muscle mechanics on human movement outcomes as
380 revealed by computer simulation." Human Movement Science **11**(3): 273-297.
- 381 Flanders, M. (1991). "Temporal patterns of muscle activation for arm movements in three-
382 dimensional space." Journal of Neuroscience **11**(9): 2680-2693.
- 383 Flanders, M., J. J. Pellegrini and S. D. Geisler (1996). "Basic features of phasic activation
384 for reaching in vertical planes." Experimental Brain Research **110**(1): 67-79.
- 385 Flanders, M., J. J. Pellegrini and J. F. Soechting (1994). "Spatial/temporal characteristics
386 of a motor pattern for reaching." Journal of Neurophysiology **71**(2): 811-813.
- 387 Flash, T. and N. Hogan (1985). "The coordination of arm movements: an experimentally
388 confirmed mathematical model." Journal of neuroscience **5**(7): 1688-1703.
- 389 Gawthrop, P. (2010). "Act-and-Wait and Intermittent Control: Some Comments." IEEE
390 Transactions on Control Systems Technology **18**(5): 1195-1198.
- 391 Gawthrop, P., I. Loram and M. Lakie (2009). "Predictive feedback in human simulated
392 pendulum balancing." Biological Cybernetics **101**(2): 131-146.
- 393 Gawthrop, P., I. Loram, M. Lakie and H. Gollee (2011). "Intermittent control: a
394 computational theory of human control." Biological Cybernetics **104**(1): 31-51.

395 Gordon, A. M., A. F. Huxley and F. J. Julian (1966). "The variation in isometric tension
396 with sarcomere length in vertebrate muscle fibres." The Journal of Physiology **184**(1): 170-
397 192.

398 Hallett, M. and C. Marsden (1979). "Ballistic flexion movements of the human thumb."
399 The Journal of Physiology **294**: 33.

400 Hallett, M., B. T. Shahani and R. R. Young (1975). "EMG analysis of stereotyped
401 voluntary movements in man." Journal of Neurology, Neurosurgery & Psychiatry **38**(12):
402 1154-1162.

403 Hanneton, S., A. Berthoz, J. Droulez and J.-J. E. Slotine (1997). "Does the brain use sliding
404 variables for the control of movements?" Biological cybernetics **77**(6): 381-393.

405 Hoffman, D. and P. Strick (1990). "Step-tracking movements of the wrist in humans. II.
406 EMG analysis." The Journal of Neuroscience **10**(1): 142-152.

407 Hoffman, D. S. and P. L. Strick (1999). "Step-Tracking Movements of the Wrist. IV.
408 Muscle Activity Associated With Movements in Different Directions." Journal of
409 Neurophysiology **81**(1): 319-333.

410 Hong, D. A., D. M. Corcos and G. L. Gottlieb (1994). "Task dependent patterns of muscle
411 activation at the shoulder and elbow for unconstrained arm movements." Journal of
412 Neurophysiology **71**(3): 1261-1265.

413 Karniel, A. (2013). "The minimum transition hypothesis for intermittent hierarchical motor
414 control." Frontiers in computational neuroscience **7**: 12.

415 Karst, G. M. and Z. Hasan (1991). "Timing and magnitude of electromyographic activity
416 for two-joint arm movements in different directions." Journal of Neurophysiology **66**(5):
417 1594-1604.

418 Lavielle, M. and E. Lebarbier (2001). "An application of MCMC methods for the multiple
419 change-points problem." Signal Processing **81**(1): 39-53.

420 Leib, R. and A. Karniel (2012). "Minimum acceleration with constraints of center of mass:
421 a unified model for arm movements and object manipulation." Journal of Neurophysiology
422 **108**(6): 1646-1655.

423 Loewenstein, Y., S. Mahon, P. Chadderton, K. Kitamura, H. Sompolinsky, Y. Yarom and
424 M. Hausser (2005). "Bistability of cerebellar Purkinje cells modulated by sensory
425 stimulation." Nat Neurosci **8**(2): 202-211.

426 Loram, I. D., H. Gollee, M. Lakie and P. J. Gawthrop (2011). "Human control of an
427 inverted pendulum: Is continuous control necessary? Is intermittent control effective? Is
428 intermittent control physiological?" The Journal of Physiology **589**(2): 307-324.

429 Miall, R., D. Weir and J. Stein (1986). "Manual tracking of visual targets by trained
430 monkeys." Behavioural brain research **20**(2): 185-201.

431 Miall, R., D. Weir and J. Stein (1987). "Visuo-motor tracking during reversible inactivation
432 of the cerebellum." Experimental Brain Research **65**(2): 455-464.

433 Moran, D. W. and A. B. Schwartz (1999). "Motor cortical representation of speed and
434 direction during reaching." Journal of neurophysiology **82**(5): 2676-2692.

435 Morasso, P. (1981). "Spatial control of arm movements." Experimental brain research
436 **42**(2): 223-227.

437 Mustard, B. E. and R. G. Lee (1987). "Relationship between EMG patterns and kinematic
438 properties for flexion movements at the human wrist." Experimental Brain Research **66**(2):
439 247-256.

- 440 Navas, F. and L. Stark (1968). "Sampling or intermittency in hand control system
441 dynamics." Biophysical Journal **8**(2): 252-302.
- 442 Neilson, P., M. Neilson and N. O'dwyer (1988). "Internal models and intermittency: a
443 theoretical account of human tracking behavior." Biological Cybernetics **58**(2): 101-112.
- 444 Norman, R. W. and P. V. Komi (1979). "Electromechanical delay in skeletal muscle under
445 normal movement conditions." Acta Physiologica Scandinavica **106**(3): 241-248.
- 446 Patla, A. E., B. S. Hudgins, P. A. Parker and R. N. Scott (1982). "Myoelectric signal as a
447 quantitative measure of muscle mechanical output." Medical and Biological Engineering
448 and Computing **20**(3): 319-328.
- 449 Sanes, J. and V. Jennings (1984). "Centrally programmed patterns of muscle activity in
450 voluntary motor behavior of humans." Experimental Brain Research **54**(1): 23-32.
- 451 Schenk, T., E. Walther and N. Mai (2000). "Closed-and open-loop handwriting
452 performance in patients with multiple sclerosis." European Journal of Neurology **7**(3): 269-
453 279.
- 454 Slifkin, A. B., D. E. Vaillancourt and K. M. Newell (2000). "Intermittency in the control
455 of continuous force production." Journal of Neurophysiology **84**(4): 1708-1718.
- 456 Squeri, V., L. Masia, M. Casadio, P. Morasso and E. Vergaro (2010). "Force-field
457 compensation in a manual tracking task." PLoS One **5**(6): e11189.
- 458 Uno, Y., M. Kawato and R. Suzuki (1989). "Formation and control of optimal trajectory in
459 human multijoint arm movement." Biological cybernetics **61**(2): 89-101.
- 460 Vaillancourt, D. E., M. A. Mayka and D. M. Corcos (2006). "Intermittent visuomotor
461 processing in the human cerebellum, parietal cortex, and premotor cortex." Journal of
462 neurophysiology **95**(2): 922-931.
- 463 Venkadesan, M. and F. J. Valero-Cuevas (2008). "Neural control of motion-to-force
464 transitions with the fingertip." Journal of Neuroscience **28**(6): 1366-1373.
- 465 Viviani, P. and C. Terzuolo (1982). "Trajectory determines movement dynamics."
466 Neuroscience **7**(2): 431-437.